Charge Hopping in Organic Semiconductors: Influence of Molecular Parameters on Macroscopic Mobilities in Model One-Dimensional Stacks

Y. Olivier,[†] V. Lemaur,[†] J. L. Brédas,[†,‡] and J. Cornil*[,†,‡]

Laboratory for Chemistry of Novel Materials, Center for Research in Molecular Electronics and Photonics, University of Mons-Hainaut, Place du Parc 20, B-7000 Mons, Belgium, and School of Chemistry and Biochemistry and Center for Organic Photonics and Electronics, Georgia Institute of Technology, Atlanta, Georgia 30332-0400

Received: December 9, 2005; In Final Form: March 22, 2006

We present a Monte Carlo approach to estimate how molecular parameters impact hopping rates and charge mobilities in organic π-conjugated materials. Our goal is to help in establishing structure−properties relationships. As a first step, our approach is illustrated by considering a model system made of a one-dimensional array of pentacene molecules; we describe the variations of the electron-transfer rates and of the resulting charge mobilities as a function of electric field and of the presence of molecular disorder and traps. The results highlight that there is no direct relationship between the degree of *spatial* overlap among adjacent molecules and charge mobility.

1. Introduction

Organic semiconductors are increasingly used as active materials in a large number of electronic devices such as light-emitting diodes, solar cells, field-effect transistors, sensors, or switches. In all cases, charge transport across organic layer(s) is playing a key role in determining device performance. Efficient charge transport is required for instance to induce the recombination of the injected electrons and holes away from the electrodes in light-emitting diodes,[1] to collect at the electrodes the charges generated upon light conversion in solar cells,[2] or to funnel charges between source and drain in transistors.[3]

The charge transport mechanism can vary as a function of temperature. In ultrapure single crystals at low temperature, a band regime can occur. In this case, the highest occupied molecular orbitals (HOMO) of the individual molecules interact to generate a valence band while interactions among the lowest unoccupied molecular orbitals (LUMO) yield a conduction band. Injected charges are then coherently delocalized over the whole crystal and are characterized by mobilities related to the HOMO and LUMO bandwidths for holes and electrons, respectively.[4] When temperature increases, lattice vibrations enhance charge scattering and effectively reduce the total bandwidths and hence charge mobilities. Thus, in a band regime, mobility decreases with temperature;[5,6] note that in the presence of traps mobility can actually increase with temperature since thermal activation helps in detrapping charges.[6]

At higher temperatures, due to the reduced effective bandwidths, the energy gained by localizing the charge carriers on single molecules can become comparable in magnitude to the energy gained by charge delocalization, thereby leading to polaron formation. The polaron binding energy comes from local geometric relaxations and increased polarization of the surrounding medium. Clearly, localization occurs in disordered materials that are in the presence of energetic disorder (that leads to a distribution of energies for the HOMO and LUMO levels as a result of changes in the conformation and/or nature of the environment of the individual molecules) and/or positional disorder (associated with fluctuations in the relative positions of the interacting molecules).[7] When localization sets in, transport operates via a hopping mechanism in which charges jump from site to site. Since organics-based devices typically operate at room temperature and incorporate inherently disordered materials, the hopping mechanism is expected to govern charge transport in most cases.

The theoretical description of charge transport via hopping in organic conjugated materials has been pioneered by the group of Bässler and co-workers[8] and has received a great deal of interest over the years. In many instances, earlier studies (i) describe the system of interest as a model lattice, thereby ignoring the actual morphology of the materials; (ii) estimate the transfer rate between adjacent sites from simple expressions (generally based on the Miller−Abrahams model)[9] that neglect polaronic effects and require input parameters that are not explicitly calculated and have to be guessed or fitted from experimental data[10−13] (in addition, these models overlook the high sensitivity of the transfer rate with respect to the relative positions of the interacting molecules); and (iii) evaluate charge propagation via Monte Carlo approaches or by solving master equations and provide in this way a *macroscopic* description of charge transport. Despite the fact that the exact chemical structures and the actual relative positions of the interacting units are not explicitly taken into account, these simulations have proven very useful; they have allowed to rationalize on a phenomenological basis the impact of multiple parameters on charge mobilities, in particular the role of energetic and positional disorder (often referred to as diagonal and nondiagonal disorder, respectively) and of applied electric field. More recent studies have also addressed the influence of charge carrier density[11,12] or of the phase separation pattern in organic blends.[13]

In this context, our recent contributions have attempted to describe charge hopping at the *molecular* level by estimating at the quantum-chemical level the main parameters controlling

[†] University of Mons-Hainaut.
[‡] Georgia Institute of Technology.

10.1021/jp0571933 CCC: $33.50
Published on Web 04/26/2006

the electron-transfer rate among interacting molecules.[14] In this way, we deal explicitly with the chemical structure of the molecules and the impact of their actual relative positions (packing). In the present work, our goal is to describe an approach to assess semiquantitatively how changes in molecular structure or packing affect charge mobilities. We describe charge transport over large distances in the presence of an electric field by inserting transfer rates computed at the quantum-chemical level for pairs of interacting molecules into Monte Carlo simulations. We illustrate this approach on model systems made of one-dimensional stacks of pentacene molecules. The choice of pentacene, though arbitrary, is motivated by the fact that it is currently one of the most studied molecular semiconductors.[15] The restriction to one-dimensional stacks allows us to rationalize easily the variations calculated in charge mobilities when (i) the relative positions of the molecules are changed, (ii) structural disorder is introduced, (iii) the external electric field is modulated, and (iv) charge traps of controlled depth are incorporated along the conduction pathway. The results we obtain are expected to be relevant to understand charge transport in quasi-one-dimensional systems such as discotic liquid crystalline phases[16,17] or nanoribbons made of conjugated oligomers.[18]

The paper is structured as follows: since we are primarily interested in the charge drift along pentacene stacks upon application of an external static electric field, we first describe Marcus theory incorporating the driving force induced by the field and the impact of the electric field on the various parameters. We then describe our Monte Carlo implementation and present the results of our simulations by illustrating the relationship between charge mobility and molecular packing, the field dependence of charge transport, and the impact of traps.

2. Theoretical Methodology

To describe charge transport along a one-dimensional stack of pentacene molecules, the key features of our approach are (i) to evaluate at the quantum-chemical level the rate of charge transfer between two adjacent molecules, in the presence of an applied external electric field, and (ii) to run Monte Carlo simulations based on the calculated transfer rates to estimate charge mobilities. These two different aspects of our theoretical approach are detailed in the next sections.

Charge-Transfer Rate between Adjacent Molecules. Marcus theory is widely used by chemists to estimate the rate of charge transfer in a weak coupling regime, which implies that the charge is localized on the donor D prior to and on the acceptor A after electron transfer: $D^- + A \rightarrow D + A^-$.[19] This formalism is readily applicable to a charge hopping process for which D and A are identical molecules. We note that Marcus theory shares many similarities with the theory of polaron hopping derived by Holstein and used mostly in the physics community.[20] In the absence of electric field, the hopping rate is generally estimated from the semiclassical formalism of Marcus as[14,21]

$$k_{hop} = \frac{2\pi}{\hbar} t^2 \frac{1}{\sqrt{4\pi\lambda k_B T}} \exp\left[-\frac{\lambda}{4k_B T}\right] \quad (1)$$

where T is the temperature, t the transfer integral that reflects the strength of electronic interaction between the adjacent molecules, and λ the total reorganization energy. The latter is made of two components: (i) the intramolecular (inner) contribution λ_i that accounts for the changes in the geometry of the two molecules upon electron transfer and (ii) the external (outer) contribution λ_s that reflects the changes in the polarization of the surrounding medium. This formalism has been recently used to estimate the mobility associated with charge diffusion in model stacks of oligophenylevinylenes (albeit in a crude way since the transfer integrals were taken to be identical for each pair of interacting molecules and λ_s was assumed to be negligible).[22]

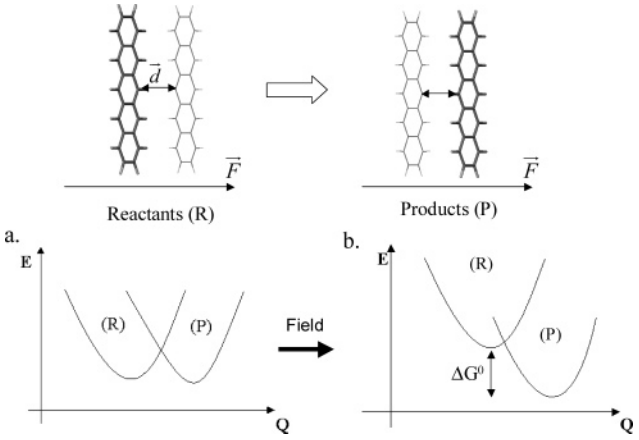

Figure 1. Illustration of the potential energy curves associated with a charge transfer from the left pentacene molecule to the right one in the absence ($\Delta G^\circ = 0$) and in the presence of an electric field ($\Delta G^\circ \neq 0$). The vectors $\vec{F}$ and $\vec{d}$ are also shown.

Equation 1 implies that (i) the reactants and products have the same energy in their equilibrium geometry (see Figure 1a; note that an applied electric field will stabilize or destabilize the products with respect to the reactants depending on its orientation and thus introduces a driving force ΔG° in the process (Figure 1b)) and (ii) the system has to reach, via thermal activation, the transition state located at the crossing between the two potential energy curves in order for charge transfer to occur. The semiclassical Marcus theory thus treats all vibrational modes classically (thus assuming that any relevant mode $\hbar\omega_i \ll k_B T$) and neglects tunneling effects across the potential barrier. The role of tunneling can be accounted for by treating selected vibrational modes at the quantum-mechanical level. This is done in our approach by adopting the Marcus−Levich−Jortner (MLJ) formalism. In that case, a single effective mode (with an energy $\hbar\omega$ set here to 0.2 eV, which is typical of C−C bond stretches) represents all the intramolecular modes and is treated quantum-mechanically via the Huang−Rhys factor S ($=\lambda_i/\hbar\omega$); the intermolecular modes are treated classically through the λ_s parameter. We note that Kumar et al. have shown that the introduction of two effective modes to describe the low- and high-frequency motions is not expected to modify significantly the calculated rates.[23] In the MLJ formalism, the transfer rate writes[24]

$$k_{hop} = \frac{2\pi}{\hbar} t^2 \sqrt{\frac{1}{4\pi\lambda_s k_B T}} \sum_{n=0}^{\infty} \exp(-S)\frac{S^n}{n!} \times \exp\left[-\frac{(\Delta G^\circ + \lambda_s + n\hbar\omega_i)^2}{4\lambda_s k_B T}\right] \quad (2)$$

where the sum runs over all pathways starting from vibrational level 0 of the reactants to vibrational level n of the products.

At the one-electron level, the application of an electric field along the stacking axis creates an energy gradient in the HOMO and LUMO levels of the individual molecules, which is assimilated here to the driving force (Figure 2). The energy

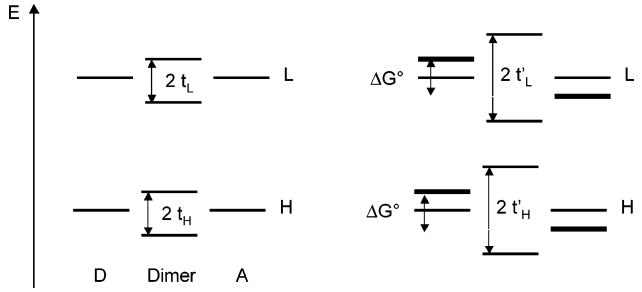

Figure 2. Energy diagram showing the way the transfer integrals are calculated in the absence of an electric field (left) and in the presence of an electric field (right). In the latter case, the introduction of a driving force $\Delta G°$ leads to apparent splittings t' larger than the effective t values (H = HOMO, L = LUMO, D = donor, A = acceptor).

difference between the HOMO/LUMO of two adjacent molecules is equal to $\Delta G° = e\cdot\vec{F}\cdot\vec{d}$ with $\vec{F}$ the vector associated with the electric field and $\vec{d}$ the vector connecting the centroid of the electronic distribution associated with the HOMO/LUMO level of the two individual molecules; in the case of symmetric molecules such as pentacene, the latter corresponds to the center of mass of the molecule. For holes [electrons], $\Delta G°$ is negative when the charges migrate along [against] the direction of the electric field and vice versa.

The internal reorganization energy λ_i of pentacene has been calculated in a previous study at the density functional theory (DFT) level using the B3LYP functional with a 6-31G(d,p) basis set.[25] It corresponds to the sum of the energies required to promote (i) the initially charged molecule from its equilibrium geometry to that characteristic of the neutral molecule and (ii) the initially neutral molecule from its equilibrium geometry to that characteristic of the radical ion. Values for λ_i of 0.095 and 0.133 eV are obtained for holes and electrons, respectively.[25] The theoretical value of λ_i for holes compares very well to the experimental value extracted from the analysis of the fine structure observed in the gas-phase ultraviolet photoelectron spectrum (UPS) of pentacene.[26] Since the electric field is consistently applied in the direction perpendicular to the molecular plane of the pentacene oligomers, the magnitude of λ_i is assumed to be field independent; this is further validated by recent calculations showing that λ_i is hardly affected in the presence of an external electric field applied along the long molecular axis of pentacene molecules.[27]

The external reorganization energy λ_s accompanying a charge-transfer process occurring in the solid state is difficult to evaluate. Simple models have been developed to estimate λ_s for a charge transfer between spherical ions in an isotropic medium.[28] On the basis of a modified expression taking into account the actual shape of the donor and acceptor molecules, values on the order of 0.3−0.4 eV are obtained when considering the dielectric characteristics of organic-based matrices.[29]

The transfer integrals can be approximated within Koopman's theorem as half the splitting of the HOMO [LUMO] levels for holes [electrons] in a complex formed by two adjacent neutral molecules.[14] They have been calculated with the help of the semiempirical Hartree−Fock intermediate neglect of differential overlap (INDO) Hamiltonian, as developed by Zerner and coworkers.[30] The energy gradient $\Delta G°$ created by the electric field introduces an energy offset between the HOMO [LUMO] levels of adjacent molecules (see Figure 2). In a two-state model, the apparent and effective splittings are related by the expression

$$2t = \sqrt{4t'^2 - (\Delta G°)^2} \qquad (3)$$

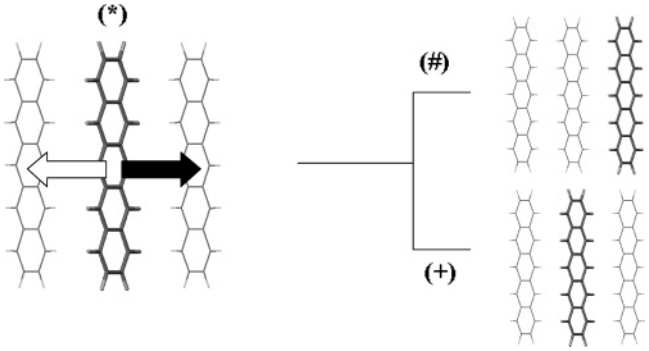

Figure 3. Illustration of the Monte Carlo algorithm: the charge is initially localized on the central pentacene molecule (*), the hopping direction is chosen randomly (it takes place to the right in this example), and the hop is either accepted (#) or rejected (+) in this iterative cycle depending on whether the acceptance condition is verified or not.

TABLE 1: Evolution of the Transfer Integral as a Function of Electric Field; Apparent t' and Effective Splittings t for Holes and Electrons as Well as the Driving Force $\Delta G°$ Introduced by the Field Are Reported

F (10^6 V/cm)	t'_{HOMO} (eV)	t'_{LUMO} (eV)	$\Delta G°$ (eV)	t_{HOMO} (eV)	t_{LUMO} (eV)
0	0.1315	0.1035	0	0.1315	0.1035
1.028	0.133	0.106	0.0411	0.1314	0.1035
2.056	0.138	0.112	0.0822	0.1312	0.1036
3.084	0.146	0.121	0.1233	0.1318	0.1035
4.112	0.155	0.133	0.1644	0.1314	0.1039
5.140	0.167	0.146	0.2055	0.1316	0.1030
6.168	0.181	0.162	0.2466	0.1318	0.1043
7.196	0.195	0.178	0.2877	0.1317	0.1040
8.224	0.211	0.195	0.3288	0.1315	0.1040
9.252	0.227	0.212	0.3699	0.1316	0.1036
10.28	0.244	0.231	0.411	0.1316	0.1044

where t' is the apparent transfer integral and t the effective value to be used in eq 2 to estimate the transfer rates. We have analyzed the field dependence of the calculated transfer integrals by computing the apparent splittings for a dimer made of two pentacene molecules separated by 4 Å, with an electric field ranging from 10^6 to 10^7 V/cm oriented perpendicular to the molecular planes (see Table 1). The effective splittings extracted with eq 3 are found to be hardly affected by the magnitude of the electric field; this can be rationalized by the fact that the electronic distributions in the HOMO or LUMO levels are only slightly perturbed for such an orientation of the electric field. As a result, the transfer integrals are kept unchanged in the Monte Carlo simulations when the magnitude of the electric field is varied.

Charge Propagation. The electron- or hole-transfer rates calculated at the quantum-chemical level are injected into Monte Carlo (MC) simulations to evaluate the propagation of a single charge along the stacks. MC methods rely on the use of random variables; in our case, the random variable is the occurrence of a hop between two adjacent molecules separated by a given distance. This distance is counted as positive if the hole propagates in the direction of the electric field and as negative in the opposite direction; this counting scheme is reversed for electrons. In the MC algorithm, the first step is to choose randomly the direction along which charge hopping takes place in a given iterative cycle (i.e., a jump either to the left or right nearest neighbor along the one-dimensional stack). This is illustrated in Figure 3 where the charge is initially located on the central molecule and where a transfer to the adjacent molecule on the right side is considered. The second step is to calculate the probability of transferring the charge in the chosen

direction as

$$p_{\rightarrow} = \frac{k_{\rightarrow}}{k_{\rightarrow} + k_{\leftarrow}} \tag{4}$$

where $k_{\rightarrow}$ and $k_{\leftarrow}$ correspond to the transfer rates in the right and left directions, respectively; these are different in the presence of the electric field. Finally, a random number is generated between 0 and 1 and is compared to $p_{\rightarrow}$. If the random number is lower than the transfer probability, the transfer in the right direction is accepted. Otherwise, the transfer is rejected; the charge carrier remains in its initial position, and a new iterative loop is performed. After a large number of iterative cycles (typically between 10^{10} and 10^{13}), the mobility can be estimated directly as

$$\mu = d/(\tau F) \tag{5}$$

with F the magnitude of the electric field, d the total distance traveled by the charge (summed as positive and negative contributions depending on the direction of the hop with respect to the field), and τ the total time calculated as the sum of the inverse of the transfer rates. The electric field has been varied here from 10^4 to 10^7 V/cm; these are reasonable values for devices a few hundred nanometers thick under the application of 10−100 V between the electrodes (we assume a linear voltage drop across the device). Thus, our approach offers a way of connecting *molecular* parameters such as λ, $\Delta G°$, and t to *macroscopic* quantities such as charge mobility. There is no limitation in size since the system is built progressively around the charge when moving down the stacks.

Since the total distance traveled by the charge is obtained as a sum of random variables, this parameter is also by definition a random variable. We have thus calculated a standard deviation on the mobility value after each hop that we express as

$$\sigma = \sqrt{\frac{1}{N}\sum_{i=1}^{N}(\mu_i - \bar{\mu})} \tag{6}$$

where N is the total number of hops since the start of the simulation, μ_i is the mobility values calculated during the simulation when the number of cycles achieved is equal to i (with i varying from 1 to N), and $\bar{\mu} = (1/N)\sum_{i=1}^{N}\mu_i$ is the average mobility obtained after N cycles. The σ value is generally less than 1% after convergence of $\bar{\mu}$ for the simulations presented in the next sections.

3. Results and Discussion

3.1. Influence of the Electric Field. We report in Figure 4 the field dependence of the hole and electron mobilities calculated for a one-dimensional array of pentacene molecules in a cofacial configuration, with an intermolecular distance fixed at 4 Å. The simulations have been performed at 300 K for an external reorganization energy of 0.4 eV. The transfer integrals associated with such an arrangement amount to 0.132 and 0.104 eV for holes and electrons, respectively (the fact that the HOMO splitting is larger than the LUMO splitting in a cofacial geometry results from the presence of a larger number of nodes in the wave function of the LUMO level compared to the HOMO level).[31] The results collected in Table 2 show that the mobility increases by about a factor of 4 for both holes and electrons when the electric field is varied from 10^4 to 10^7 V/cm. Since the magnitude of the electric field appears in the denominator of the mobility expression (eq 5), the results further indicate

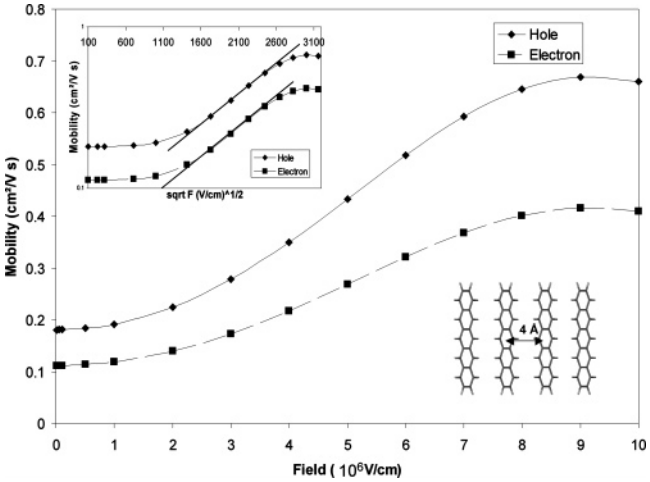

Figure 4. Evolution of the hole mobility as a function of the magnitude of the electric field in a one-dimensional array of pentacene molecules separated by 4 Å. The inset illustrates the evolution as a function of the square root of the electric field.

that the charge velocity (d/τ) increases faster than the magnitude of the field. The ratio between the hole and electron mobilities at any field perfectly matches the ratio of the corresponding transfer rates. Despite the fact that a direct comparison cannot be made between experimental data and our model systems which are restricted to one-dimensional stacks, it is interesting to note that the calculated mobility values (in the range 10^{-1}−1 cm^2/(V s)) are very reasonable; the mobilities reported for pentacene thin films and crystals are usually in the range 0.1−5 cm^2/(V s).[32]

The evolution of the mobility at lower field can be fitted by a Poole−Frenkel- like expression[32]

$$\mu = \mu_0 \exp(\gamma\sqrt{F}/kT) \tag{7}$$

with the constant γ estimated to be 8×10^{-4} eV(cm/V)$^{1/2}$ for both holes and electrons. Interestingly, the mobility values start deviating from this expression and pass by a maximum for an electric field close to 10^7 V/cm. This actually occurs when the charge velocity increase becomes smaller than that of the electric field; this happens as the inverted regime of Marcus theory is approached (that is, at the semiclassical level, when $\Delta G° > \lambda$); in that regime, any further increase in driving force leads to a reduction in transfer rate and hence in mobility. Such a decrease in mobility with electric field has been calculated in previous studies,[8,34,35] for instance, by Garstein and Conwell,[34] who considered spatially correlated energetic disorder.

3.2. Influence of the Reorganization Energy. Since the external reorganization energy may vary significantly in specific cases (for instance, when the molecules are located close to structural defects or in the vicinity of metallic electrodes), we have investigated the way the hole mobility evolves as a function of the magnitude of λ_s. The Monte Carlo simulations have been performed on the same one-dimensional array of pentacene molecules as discussed earlier, with an electric field fixed at 5×10^6 V/cm and at 300 K. Figure 5 illustrates the mobility drop with λ_s. The mobility is reduced by about a factor of 5 for an increase of λ_s from 0.2 to 0.4 eV or from 0.4 to 0.6 eV; it is strongly hampered beyond 0.7 eV. In this case, the evolution simply reflects that for the transfer rate (see inset of Figure 5).

3.3. Influence of Intermolecular Distance. Changes in the distance between molecules can be modulated by substituents attached to conjugated backbones. Accordingly, we have examined the evolution of hole mobility in the one-dimensional

TABLE 2: Evolution with Electric Field Magnitude of the Transfer Rates in the Directions Parallel ($k_{\rightarrow}$) and Opposite ($k_{\leftarrow}$) to the Field and of the Corresponding Mobilities for Hole and Electron Transport

F (10^6 V/cm)	$k_{\rightarrow}$(hole) (s^{-1})	$k_{\leftarrow}$(hole) (s^{-1})	μ_{hole} (cm^3/V s)	$k_{\leftarrow}$(electron) (s^{-1})	$k_{\rightarrow}$(electron) (s^{-1})	$\mu_{electron}$ (cm^2/(V s))
0.01	5.89×10^{12}	5.80×10^{12}	0.18	3.65×10^{12}	3.59×10^{12}	0.11
0.05	6.07×10^{12}	5.62×10^{12}	0.18	3.76×10^{12}	3.48×10^{12}	0.11
0.1	6.31×10^{12}	5.40×10^{12}	0.18	3.91×10^{12}	3.35×10^{12}	0.11
0.5	8.52×10^{12}	3.93×10^{12}	0.18	5.28×10^{12}	2.43×10^{12}	0.11
1	1.22×10^{13}	2.59×10^{12}	0.19	7.56×10^{12}	1.61×10^{12}	0.12
2	2.35×10^{13}	1.06×10^{12}	0.22	1.46×10^{13}	6.59×10^{11}	0.14
3	4.22×10^{13}	4.04×10^{11}	0.28	2.63×10^{13}	2.51×10^{11}	0.17
4	7.02×10^{13}	1.42×10^{11}	0.35	4.36×10^{13}	8.83×10^{10}	0.22
5	1.08×10^{14}	4.63×10^{10}	0.43	6.72×10^{13}	2.88×10^{10}	0.27
6	1.55×10^{14}	1.40×10^{10}	0.52	9.64×10^{13}	8.68×10^{9}	0.32
7	2.07×10^{14}	3.91×10^{9}	0.59	1.29×10^{14}	2.43×10^{9}	0.37
8	2.58×10^{14}	1.01×10^{9}	0.65	1.60×10^{14}	6.27×10^{8}	0.40
9	3.01×10^{14}	2.42×10^{8}	0.67	1.87×10^{14}	1.50×10^{8}	0.42
10	3.30×10^{14}	5.35×10^{7}	0.66	2.05×10^{14}	3.32×10^{7}	0.41
11	3.43×10^{14}	1.10×10^{7}	0.62	2.13×10^{14}	6.81×10^{6}	0.39
12	3.38×10^{14}	2.09×10^{6}	0.56	2.01×10^{14}	1.29×10^{6}	0.35

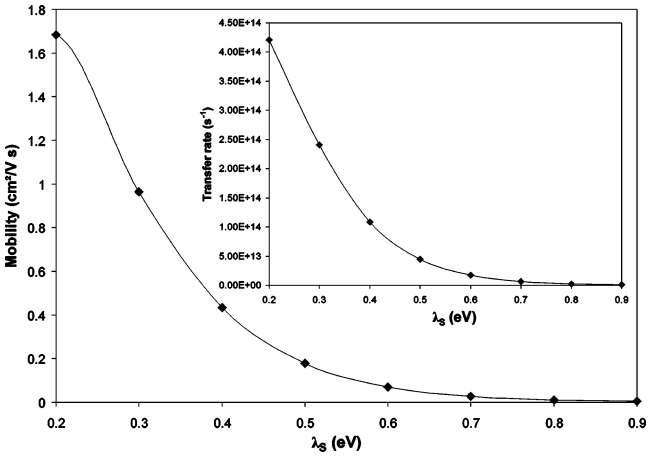

Figure 5. Evolution of the hole mobility as a function of the magnitude of the external reorganization energy in a one-dimensional array of pentacene molecules separated by 4 Å.

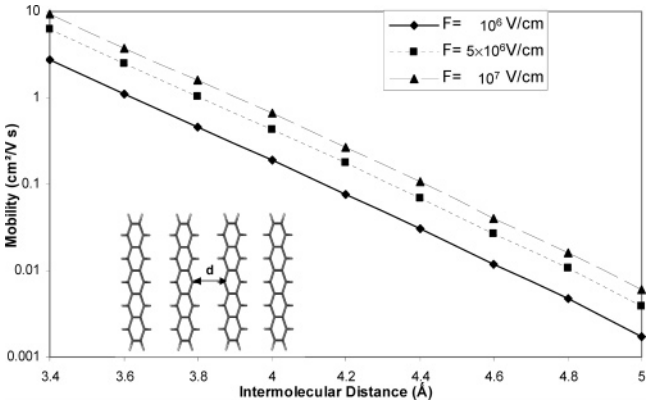

Figure 6. Evolution of the hole mobility as a function of intermolecular distance in a one-dimensional array of pentacene molecules.

array of pentacene molecules when varying the intermolecular separation between 3.4 and 5 Å (see Figure 6). In the remainder, unless stated otherwise, the simulations have been achieved with $\lambda_s = 0.4$ eV and for three different magnitudes of the electric field (10^6, 5×10^6, and 10^7 V/cm). In all cases, the mobility drops exponentially with an increase in the intermolecular distance and is shifted rigidly depending on the magnitude of the electric field; this evolution has to be traced back to that of the transfer integrals since the overlap between the HOMOs decreases exponentially with distance.

3.4. Influence of Molecular Translations. We have looked at the impact of translating molecules in a direction either parallel or perpendicular to the stacking axis. Figure 7 shows the variation of the hole mobility when translating every other molecule by a distance *d* perpendicularly to the stacking axis (note a single transfer integral value characterizes the full system). The conventional wisdom here would be that the mobility goes down with an increase in displacement due to the progressive reduction in *spatial* overlap between two adjacent molecules. However, as shown earlier,[31] the calculated values do globally decrease with distance *but* in an oscillating way. This evolution fully reflects that of the corresponding transfer integrals.

Once again, we emphasize that it is the balance between the number of bonding vs antibonding interactions in the *electronic* overlap between the wave functions of the two molecules that dictates the magnitude of the transfer integral and thus of the hole mobility. Maxima are observed when one kind of interactions dominates and minima when there occurs a compensation between them.

We have also shifted every other molecule along the stacking axis by a distance ranging from 0.1 to 0.5 Å with respect to the initial situation where all the molecules are separated by 4 Å. In such an arrangement, the charge has to hop alternatively over a distance larger and shorter than 4 Å. For various magnitudes of the applied electric field, we obtain parallel variations that point to a reduction in the mobility when the displacement is amplified (Figure 8); the impact is much more pronounced for large shifts. This behavior can be understood by comparing the transfer rates associated with the short and long hops. When the distance is smaller [longer] than 4 Å, the transfer rate increases [decreases], as discussed in section 3.3. However, since the evolution with respect to the initial distance is not symmetric (see Table 3), the time required to make two consecutive hops in the same direction (and thus to travel in all cases a distance of 8 Å) increases with the degree of translation. Interestingly, fluctuations in the separation as large as 0.5 Å do reduce the mobility by only a factor of 5.

3.5. Introduction of a Gaussian Disorder. We generalize the simulations carried out in the previous section by introducing a Gaussian distribution of the intermolecular distances d along the cofacial stack, randomly among the pairs of interacting molecules. The corresponding transfer integrals are estimated from an analytical expression of the results obtained in section 3.3:

$$t\,(\mathrm{eV}) = 646.617 \exp(-2.125d)$$

with *d* the intermolecular distance; we further assume here that

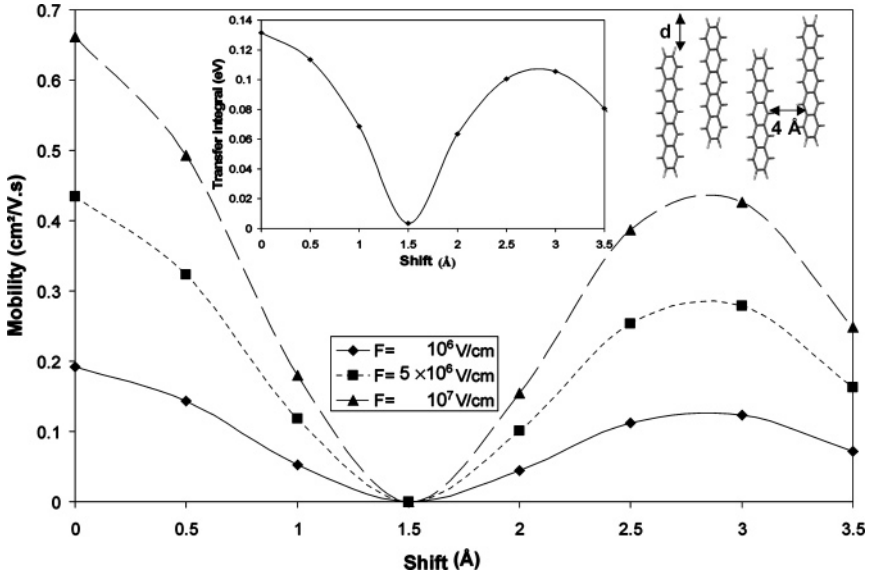

Figure 7. Evolution of the hole mobility as a function of the shift applied to every other molecule in a direction perpendicular to the stacking axis in a one-dimensional array of pentacene molecules separated by 4 Å. The inset shows the evolution of the corresponding transfer integral.

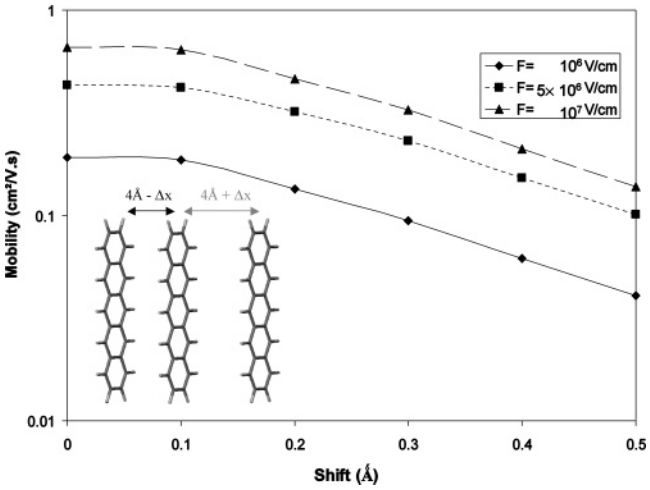

Figure 8. Evolution of the hole mobility as a function of the shift applied to every single molecule over two in a direction parallel to the stacking axis.

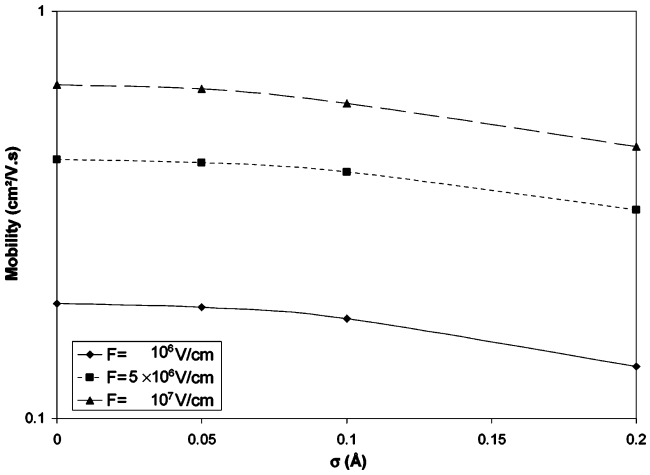

Figure 9. Evolution of the hole mobility as a function of the width of the Gaussian distribution of the intermolecular distances in the one-dimensional array of pentacene molecules.

TABLE 3: Parameters Characterizing Hole Transport at a Field of 10^6 V/cm in a One-Dimensional System Where Every Other Molecule Is Translated along the Stacking Axis Direction[a]

Δx (Å)	$k_{4Å-\Delta x}$ (s^{-1})	$k_{4Å+\Delta x}$ (s^{-1})	time for 8 Å (s)	μ (cm^2/(V s))
0	1.22×10^{13}	1.22×10^{13}	1.64×10^{-13}	0.19
0.1	1.86×10^{13}	8.68×10^{12}	1.69×10^{-13}	0.19
0.2	2.83×10^{13}	5.09×10^{12}	2.32×10^{-13}	0.13
0.3	4.28×10^{13}	3.29×10^{12}	3.28×10^{-13}	0.09
0.4	6.44×10^{13}	2.08×10^{12}	4.95×10^{-13}	0.06
0.5	9.63×10^{13}	1.36×10^{12}	7.47×10^{-13}	0.04

[a] We report in the columns the displacement, the transfer rate for the short and long hops, the time for two consecutive hops, and the hole mobility.

λ_s is not affected by variations in the intermolecular distances. The Gaussian distribution is centered around an average value m set equal to 4 Å and is characterized by a standard deviation σ set equal to 0.05, 0.1, and 0.2 Å, respectively, in the simulations:

$$g(d) = \frac{1}{\sigma\sqrt{2\pi}} \exp\left[-\frac{(d-m)^2}{2\sigma^2}\right] \qquad (8)$$

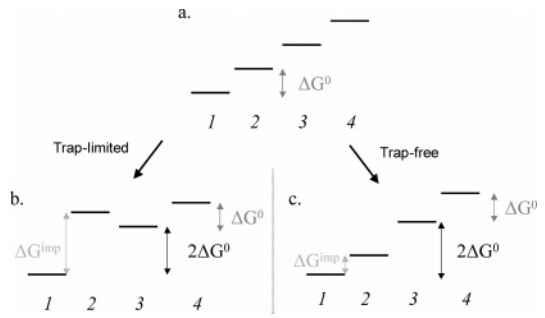

Figure 10. Energy diagram illustrating the energy gradient induced by the electric field along the one-dimensional stack (a) and the introduction of an impurity associated with a ΔG^{imp} parameter. Different situations can be encountered depending on the magnitude of the electric field and hence of $\Delta G°$: (b) $\Delta G^{imp} > 2\Delta G°$, implying that the HOMO level of the impurity acts as a trap; (c) $0 < \Delta G^{imp} < 2\Delta G°$; and (d) $\Delta G^{imp} = 0$.

With this expression, 99% of the generated distances lie in the interval $[m - 3\sigma, m + 3\sigma]$. Figure 9 shows that, as expected, the mobility is reduced when the standard deviation increases, whatever the magnitude of electric field. However, this reduction is very moderate and points to the weak impact of such types

TABLE 4: Evolution of the Hole Mobility and Time Spent on the Impurity as a Function of ΔG^{imp}

ΔG^{imp} (eV)	μ_1 (cm^3/(V s))	μ_2 (cm^3/(V s))	time on the impurity$_1$[a] (s)	time on the imurity$_2$[a] (s)
0	0.1921	0.4266	9.28×10^{-13}	3.82×10^{-13}
0.1	0.1916	0.4330	1.33×10^{-12}	9.91×10^{-14}
0.2	0.1701	0.4339	2.61×10^{-11}	6.45×10^{-14}
0.3	0.0301	0.4330	1.09×10^{-9}	9.93×10^{-14}
0.4	7.29×10^{-4}	0.4261	5.28×10^{-8}	3.95×10^{-13}
0.5	1.36×10^{-5}	0.3589	2.83×10^{-6}	3.93×10^{-12}
0.6	2.17×10^{-7}	0.0775	1.79×10^{-4}	8.58×10^{-11}

[a] The indices 1 and 2 correspond to the two different electric fields (10^6 and 5×10^6 V/cm, respectively).

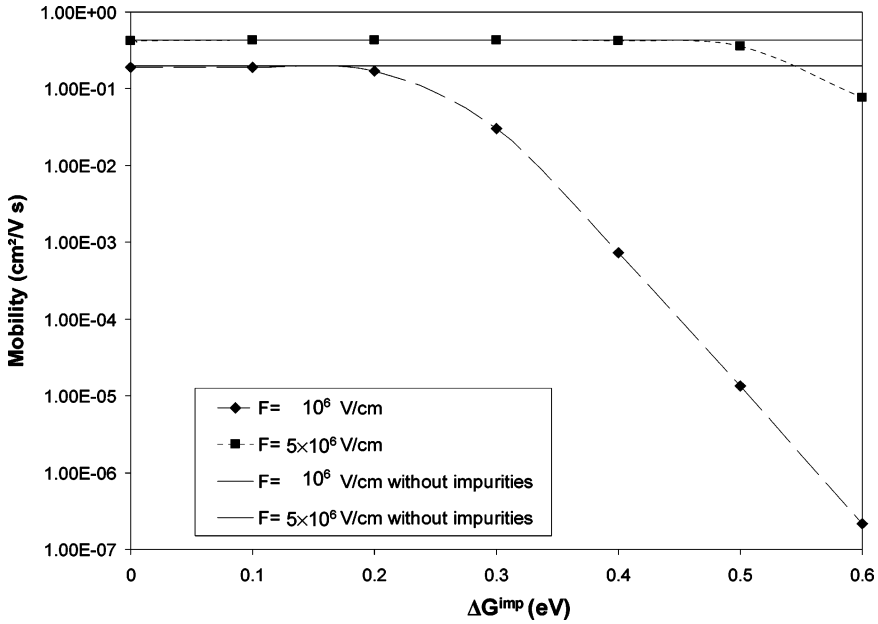

Figure 11. Evolution of the hole mobility as a function of ΔG^{imp} when one impurity is introduced per 1000 pentacene molecules. The solid lines represent the hole mobility in the absence of the impurity for the two different electric fields.

of fluctuations on charge transport properties. The calculated evolution is due to the fact that the transfer rate increases faster below 4 Å than it decreases above 4 Å. The field dependence of the mobility also exhibits a Poole−Frenkel behavior with a deviation at high field and a γ coefficient similar to that estimated for the perfectly ordered stack.

3.6. Introduction of Impurities. Finally, we have analyzed the impact of introducing impurities along the one-dimensional stack. The nature of some impurities has been established for pentacene (for instance, 6,13-dihydropentacene or pentacenequinone).[36,37] However, impurities have been described here in a generalized way and treated as molecules that break the regular energy gradient induced by the electric field, as illustrated in Figure 10a. In our simulations, an impurity is associated with a driving force equal to ΔG^{imp} for a hole hopping from the left side and ($\Delta G^{imp} - 2\Delta G°$) for hopping from the right side. (We note that, to a first approximation, we have taken λ_i and λ_s to be the same for the impurity and for the pentacene molecules.) Two different situations can be encountered depending on the magnitude of the electric field and hence of $\Delta G°$: (i) $\Delta G^{imp} > 2\Delta G°$, which implies that the HOMO level of the impurity acts as a trap (see Figure 10b), and (ii) $0 < \Delta G^{imp} < 2\Delta G°$ (see Figure 10c). We have run the simulations for two different magnitudes of the electric field (10^6 and 5×10^6 V/cm), leading to $\Delta G°$ values of 0.04 and 0.20 eV, respectively. ΔG^{imp} has been varied from 0.0 to 0.6 eV, with a density of impurities set initially to one per 1000 pentacene molecules.We depict in Figure 11 the variation of the hole mobility as a function of ΔG^{imp} at 300 K. The results indicate that the mobility value drops abruptly beyond a threshold value of ΔG^{imp}; as expected, this threshold shifts toward larger ΔG^{imp} values when the magnitude of the electric field is increased. Below the threshold, the electronic structure characteristics of the stack incorporating the impurities is shown by Figure 10c. In this regime, the hole mobility is slightly affected by the actual position of the HOMO level of the impurity though a somewhat larger value is calculated when ΔG^{imp} is exactly equal to $\Delta G°$. We stress that at room temperature the threshold significantly deviates from twice the value of $\Delta G°$. This is evidenced by the fact that the mobility value calculated at lower field for $\Delta G^{imp} = 0.2$ eV (while $\Delta G° = 0.04$ eV) relates to the situation depicted in Figure 10b but almost lies in the plateau region in Figure 11. The threshold converges toward $2\Delta G°$ when the temperature decreases.

We have plotted in Figure 12 the time spent on the impurity, defined as the time needed in the simulation to go from its left side to the first molecule on its right side; the values have been averaged over more than 10^{10} simulations. We clearly see in the plot associated with the largest electric field that the time is smallest when ΔG^{imp} is equal to 0.2 eV (i.e., when the hops around the impurity are fully symmetric), in agreement with our discussion in previous sections. We have also performed a series of simulations at an electric field of 10^6 V/cm with a ΔG^{imp} value of 0.2 eV for various densities in impurities (from 0.1 to 100 impurities for per 1000 pentacene molecules) (see Figure 13). As expected, the mobility decreases with impurity density; however, the reduction is only of 1 order of magnitude between the two limiting cases considered here.

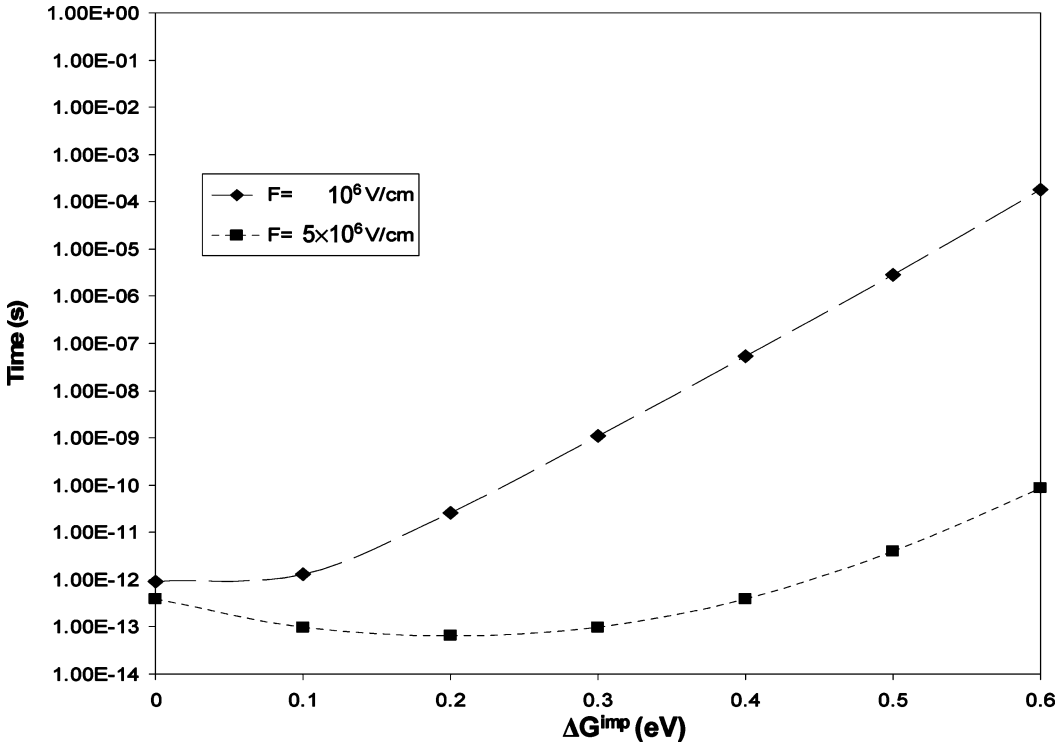

Figure 12. Evolution of the time spent by the hole around the impurity as a function of ΔG^{imp} when one impurity is introduced per 1000 pentacene molecules.

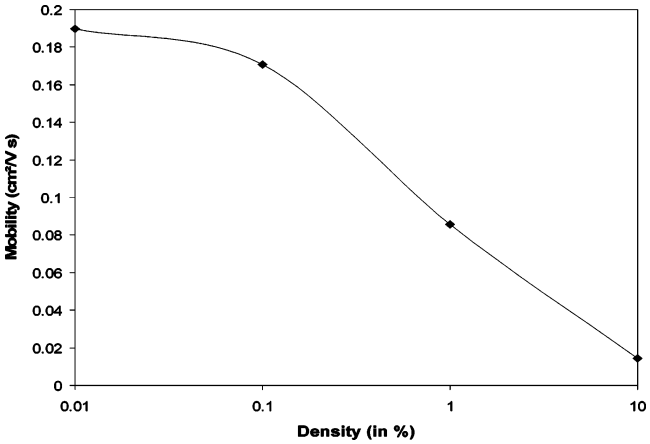

Figure 13. Evolution of the hole mobility as a function of the density in impurities for an electric field of 10^6 V/cm and $\Delta G^{imp} = 0.2$ eV.

4. Conclusions

We have combined a Monte Carlo approach to quantum-chemical calculations to estimate charge mobilities in organic materials on the basis of electron-transfer rates estimated at the molecular level. This approach allows us to describe the impact of spatial and energetic disorder and traps on the charge transport properties. For the sake of illustration, this approach has been applied here to model one-dimensional stacks of pentacene molecules. The results highlight the full parallelism between the variation of the transfer integrals at the *microscopic* scale and that of the charge mobilities at the *macroscopic* scale when the relative positions of the interacting molecules are modulated along the one-dimensional stacks. They also confirm the absence of direct relationship between the degree of *spatial* overlap between adjacent molecules and the charge mobility. The field dependence of the mobility is found to follow a Poole−Frenkel law in a limited range of applied electric field, both in the absence and in the presence of molecular disorder. Our approach is currently being extended to consider two- and three-dimensional systems and to incorporate electron−electron interaction effects.

Acknowledgment. This paper is dedicated to Professor Bob Silbey on the occasion of his 65th birthday. The authors, who represent three generations of Silbey students and collaborators, are immensely grateful to Bob for the many stimulating discussions over the years and his continuous interest in our research activities. The work in Mons is partly supported by the Belgian Federal Governement "Interuniversity Attraction Pole in Supramolecular Chemistry and Catalysis, PAI 5/3"; Région Wallonne (Project ETIQUEL); the European Integrated Project project NAIMO (NMP4-CT-2004-500355); and the Belgian National Fund for Scientific Research (FNRS/FRFC). The work at Georgia Tech is partly supported by the National Science Foundation (through grant CHE-0342321 and CRIF award CHE-0443564) and the Office of Naval Research. J.C. is an FNRS Research Fellow; V.L. and Y.O. acknowledge a grant from "Fonds pour la Formation à la Recherche dans l'Industrie et dans l'Agriculture (FRIA)".

References and Notes

(1) Friend, R. H.; Gymer, R. W.; Holmes, A. B.; Burroughes, J. H.; Marks, R. N.; Taliani, C.; Bradley, D. D. C.; dos Santos, D. A.; Brédas, J. L.; Lögdlund, M.; Salaneck, W. R. *Nature (London)* **1999**, *397*, 121.

(2) Brabec, C. J.; Sariciftci, N. S.; Hummelen, J. C. *Adv. Funct. Mater.* **2001**, *11*, 15.

(3) Horowitz, G. *Adv. Mater.* **1998**, *10*, 365.

(4) Siegrist, T.; Fleming, R. M.; Haddon, R. C.; Laudise, R. A.; Lovinger, A. J.; Katz, H. E.; Bridenbaugh, P.; Davis, D. D. *J. Mater. Res.* **1995**, *10*, 2170.

(5) Karl, N. *Synth. Met.* **2003**, *133*−*134*, 649.

(6) Podzorov, V.; Menard, E.; Borissov, A.; Kiryukhin, V.; Rogers, J. A.; Gershenson, M. E. *Phys. Rev. Lett.* **2004**, *93*, 086602.

(7) Kang, J. H.; da Silva Filho, D. A.; Brédas, J. L.; Zhy, X. Y. *Appl. Phys. Lett.* **2005**, *86*, 152115.

(8) Bässler, H. *Phys. Status Solidi B* **1993**, *175*, 15.
(9) Miller, A.; Abrahams, E. *Phys. Rev.* **1960**, *120*, 45.
(10) Offermans, T.; Meskers, S. C. J.; Janssen, R. A. J. *Chem. Phys.* **2005**, *308*, 125.
(11) Pasveer, W. F.; Cottaar, J.; Tanase, C.; Coehoorn, R.; Bobbert, P. A.; Blom, P. W. M.; de Leeuw, D. M.; Michels, M. A. J. *Phys. Rev. Lett.* **2005**, *94*, 206601.
(12) Coehoorn, R.; Pasveer, W. F.; Bobbert P. A.; Michels, M. A. J. *Phys. Rev. B* **2005**, *72*, 1.
(13) Chatten, A. J.; Tuladhar, S. M.; Choulis, S. A.; Bradley, D. D. C.; Nelson, J. *J. Mater. Sci.* **2005**, *40*, 1393.
(14) Brédas, J. L.; Beljonne, D.; Coropceanu, V.; Cornil, J. *Chem. Rev.* **2004**, *104*, 4971.
(15) Ruiz, R.; Choudhary, D.; Nickel, B.; Toccoli, T.; Chang, K. C.; Mayer, A. C.; Clancy, P.; Blakely, J. M.; Headrick, R. L.; Iannotta, S.; Malliaras, G. G. *Chem. Mater.* **2004**, *16*, 4497.
(16) Adam, D.; Schuhmacher, P.; Simmerer, J.; Häussling, L.; Siemensmeyer, K.; Etzbach, K. H.; Ringsdorf, H.; Haarer, D. *Nature (London)* **1994**, *371*, 141.
(17) Lemaur, V.; da Silva Filho, D. A.; Coropceanu, V.; Lehmann, M.; Geerts, Y.; Piris, J.; Debije, M. G.; van de Craats, A. M.; Senthilkumar, K.; Siebbeles, L. D. A.; Warman, J. M.; Brédas, J. L.; Cornil, J. *J. Am. Chem. Soc.* **2004**, *126*, 3271.
(18) Leclère, Ph.; Surin, M.; Jonkheijm, P.; Henze, O.; Schenning, A. P. H. J.; Biscarini, F.; Grimsdale, A. C.; Feast, W. J.; Meijer, E. W.; Müllen, K.; Brédas, J. L.; Lazzaroni, R. *Eur. Polym. J.* **2004**, *40*, 885.
(19) Marcus, R. A. *Rev. Mod. Phys.* **1993**, *65*, 599.
(20) Holstein, T. *Ann. Phys.* **1959**, *8*, 325.
(21) Chatten, A. J.; Tuladhar, S. M.; Choulis, S. A.; Bradley, D. D. C.; Nelson, J. *J. Mater. Sci.* **2004**, *40*, 1393.
(22) Prins, P.; Senthkumar, K.; Grozema, F. C.; Jonkheijm, P.; Schenning, A. P. H. J.; Meijer, E. W.; Siebbeles, L. D. A. *J. Phys. Chem. B* **2005**, *109*, 18267.
(23) Kumar, K.; Kurnikov, I. V.; Beratan, D.; Waldeck, D. H.; Zimmt, M. B. *J. Phys. Chem. A* **1998**, *102*, 5529.
(24) Jortner, J. *J. Chem. Phys.* **1976**, *64*, 4860.
(25) Coropceanu, V.; Malagoli, M.; de Silva Filho, D. A.; Gruhn, N. E.; Bill, T. G.; Brédas, J. L. *Phys. Rev. Lett.* **2002**, *89*, 275503.
(26) Gruhn, N. E.; da Silva Filho, D. A.; Bill, T. G.; Malagoli, M.; Coropceanu, V.; Kahn, A.; Brédas, J. L. *J. Am. Chem. Soc.* **2002**, *124*, 7918.
(27) Sancho-Garcia, J. C.; Horowitz, G.; Brédas, J. L.; Cornil, J. *J. Chem. Phys.* **2003**, *119*, 12563.
(28) Marcus, R. A. *J. Chem. Phys.* **1965**, *43*, 679.
(29) Lemaur, V.; Steel, M. C.; Beljonne, D.; Brédas, J. L.; Cornil, J. *J. Am. Chem. Soc.* **2005**, *127*, 6077.
(30) Zerner, M. C.; Loew, G. H.; Kichner, R. F.; Mueller-Westerhoff, U. T. *J. Am. Chem. Soc.* **1980**, *102*, 589.
(31) Brédas, J. L.; Calbert, J. P.; da Silva Filho, D. A.; Cornil, J. *Proc. Natl. Acad. Sci. U.S.A.* **2002**, *99*, 5804.
(32) Facchetti, A.; Yoon, M. H.; Marks, T. J. *Adv. Mater.* **2005**, *17*, 1705.
(33) Borsenberger, P. M.; Weiss, D. S. In *Organic Photoreceptors for Imaging Systems*; Marcel Dekker: New York, 1993.
(34) Garstein, Y. N.; Conwell, E. M. *Chem. Phys. Lett.* **1995**, *245*, 351.
(35) Novikov, S. V.; Dunlap, D. H.; Kenkre, V. M.; Parris, P. E.; Vannikov, A. V. *Phys. Rev. Lett.* **1998**, *81*, 4472.
(36) Jurchescu, O. D.; Baas, T.; Palstra, T. T. M. *Appl. Phys. Lett.* **2004**, *84*, 3061.
(37) Northrup, J. E.; Chabinyc, M. L. *Phys. Rev. B* **2003**, *68*, 041202.